Featured Article

Combined Epidermal Growth Factor Receptor Targeting with the Tyrosine Kinase Inhibitor Gefitinib (ZD1839) and the Monoclonal Antibody Cetuximab (IMC-C225): Superiority Over Single-Agent Receptor Targeting

Pablo Matar,[1] Federico Rojo,[2] Raúl Cassia,[3] Gema Moreno-Bueno,[3] Serena Di Cosimo,[4] José Tabernero,[1] Marta Guzmán,[1] Sonia Rodriguez,[1] Joaquín Arribas,[1] José Palacios,[3] and José Baselga[1]

[1]Laboratory of Oncology Research, Medical Oncology Service, and [2]Pathology Service, Vall d'Hebron University Hospital, Barcelona, Spain; [3]Laboratory of Breast and Gynecological Cancer, Molecular Pathology Program, Centro Nacional de Investigaciones Oncológicas (CNIO), Madrid, Spain; and [4]Division of Medical Oncology "A", Regina Elena Cancer Institute, Rome, Italy

ABSTRACT

Purpose: **The epidermal growth factor receptor (EGFR) is abnormally activated in cancer and two classes of anti-EGFR agents, monoclonal antibodies and low-molecular-weight tyrosine kinase inhibitors, have shown antitumor activity in patients. Because these two classes of antireceptor agents target the EGFR at different sites, we decided to explore whether the combined administration of gefitinib, a tyrosine kinase inhibitor, and cetuximab, a monoclonal antibody, had superior antitumor activity than either agent given alone.**

Experimental Design: **We studied the effects of the combination of gefitinib and cetuximab in a panel of human cancer cell lines and in an EGFR-dependent human tumor xenograft model (A431). The effects of these two agents on EGFR signaling, proliferation, apoptosis, and vascularization were evaluated. In addition, we analyzed, with cDNA arrays, changes in gene expression profiles induced by both agents.**

Results: **The combined treatment with gefitinib and cetuximab resulted in a synergistic effect on cell proliferation and in superior inhibition of EGFR-dependent signaling and induction of apoptosis. In a series of *in vivo* experiments, single-agent gefitinib or cetuximab resulted in transient complete tumor remission only at the highest doses. In contrast, suboptimal doses of gefitinib and cetuximab given together resulted in a complete and permanent regression of large tumors. In the combination-treated tumors, there was a superior inhibition of EGFR, mitogen-activated protein kinase, and Akt phosphorylation, as well as greater inhibition of cell proliferation and vascularization and enhanced apoptosis. Using cDNA arrays, we found 59 genes that were coregulated and 45 genes differentially regulated, including genes related to cell proliferation and differentiation, transcription, DNA synthesis and repair, angiogenesis, signaling molecules, cytoskeleton organization, and tumor invasion and metastasis.**

Conclusions: **Our findings suggest both shared and complementary mechanisms of action with gefitinib and cetuximab and support combined EGFR targeting as a clinically exploitable strategy.**

INTRODUCTION

The epidermal growth factor receptor (EGFR) is a member of the ErbB family of receptors that is abnormally activated in many epithelial tumors. This receptor family comprise four related receptors: the epidermal growth factor receptor itself (EGFR/ErbB1), ErbB2 (HER2/*neu*), ErbB3, and ErbB4 (1). Activation of the EGFR protein tyrosine kinase results in the recruitment and phosphorylation of several intracellular substrates. A major downstream signaling route of the EGFR family is via the Ras–Raf–mitogen-activated-protein-kinase-(MAPK) pathway. Activation of Ras initiates a multistep phosphorylation cascade that leads to the activation of MAPKs, ERK1, and ERK2. ERK1/2 regulate transcription of molecules that are linked to cell proliferation, survival, and transformation. Another important target in EGFR signaling is phosphatidylinositol 3-kinase (PI3K) and the downstream protein-serine/threonine kinase Akt. Akt transduces signals that trigger a cascade of responses from cell growth and proliferation to survival and motility (2).

There is strong evidence in support of targeting the EGFR as cancer therapy: the EGFR is frequently overexpressed and/or abnormally activated in tumors; receptor overexpression correlates with a worse outcome; and early studies with anti-EGFR monoclonal antibodies directed at the EGFR were shown to

Received 5/3/04; revised 5/20/04; accepted 5/26/04.
Grant support: Supported in part by Spanish Science and Technology Ministry grant SAF2003-03818 (J. Baselga) and by an unrestricted research grant from AstraZeneca, Spain. P. Matar is the recipient of a postdoctoral fellowship grant from "Fundación Carolina," Spain. S. Di Cosimo is a recipient of a research fellowship grant by the Italian Association of Medical Oncology (AIOM).
The costs of publication of this article were defrayed in part by the payment of page charges. This article must therefore be hereby marked *advertisement* in accordance with 18 U.S.C. Section 1734 solely to indicate this fact.
Requests for reprints: José Baselga, Medical Oncology Service, Vall d'Hebron University Hospital, Paseo Vall d'Hebron 119-129, Barcelona 08035, Spain. Phone: 34-93-274-6077; Fax: 34-93-274-6059; E-mail: jbaselga@vhebron.net.

inhibit the growth of cancer cells bearing the EGFR (for review of the rationale, see ref. 3). Two main anti-EGFR strategies are currently in clinical development: monoclonal antibodies that are directed at the ligand-binding extracellular domain and that prevent ligand binding and ligand-dependent receptor inhibition; and low-molecular-weight tyrosine kinase inhibitors that compete with ATP for binding to the tyrosine kinase portion of the receptor. These two classes of agents have shown solid preclinical and clinical activity in a variety of tumor types (for review, see ref. 4).

An important question is whether the monoclonal antibodies and the low-molecular-weight tyrosine kinase inhibitors, share similar mechanisms of action that could potentially make them interchangeable or whether, on the contrary, they have substantial mechanistic differences that could be exploited clinically. At first glance, these two classes of agents have similar mechanisms of action: they prevent ligand-induced receptor activation and block signaling of EGFR-dependent pathways. There is, however, evidence that some of their mechanisms of action and their antitumor effects are not completely overlapping. Anti-EGFR monoclonal antibodies, but not the low-molecular-weight tyrosine kinase inhibitors, have the capacity to form receptor-containing complexes that result in receptor internalization, an important mechanism for attenuating receptor signaling (5). In addition, anti-EGFR monoclonal antibodies can elicit antibody-dependent cellular cytotoxicity (ADCC; ref. 6). On the other hand, the low-molecular-weight EGFR tyrosine kinase inhibitors can induce the formation of inactive EGFR homodimers and EGFR/HER2 heterodimers, which impair EGFR-mediated transactivation of the potent HER2 tyrosine kinase (7–9). In terms of their antiproliferative effects, we had previously reported, in cultured cancer cells inhibited by low-molecular-weight EGFR tyrosine kinase inhibitors, that the addition of monoclonal antibodies can result in further antitumor activity (10). In addition, emerging data from the clinic suggest that these agents have different activity profiles (11, 12).

On the basis of these considerations supporting the hypothesis that these two classes of anti-EGFR strategies have complementary mechanisms of action, we decided to study and characterize the effects of the combined treatment with cetuximab, an anti-EGFR monoclonal antibody, and gefitinib, an oral low-molecular-weight tyrosine kinase inhibitor of the EGFR. These two agents, cetuximab and gefitinib, were chosen because they have been extensively studied in the laboratory and they are in advanced clinical development (for review, see ref. 4). We have studied the effects of the combination of cetuximab and gefitinib on human cancer cell lines and in an EGFR-dependent human tumor xenograft model. We have also evaluated the effects of these two agents on receptor signaling, proliferation, apoptosis, and vascularization. Finally, to further define the differences between gefitinib and cetuximab we have analyzed, using cDNA arrays, changes in gene expression profiles induced by both agents.

MATERIALS AND METHODS

Compounds. EGFR-tyrosine kinase inhibitor gefitinib (ZD1839; Iressa; kindly provided by AstraZeneca Pharmaceuticals, Macclesfield, United Kingdom) and monoclonal antibody anti-EGFR cetuximab (IMC-C225; Erbitux; kindly provided by Merck KGaA, Darmstadt, Germany) were used for *in vitro* and *in vivo* assays. The primary antibodies used for Western blot assays were as follows: rabbit polyclonal phospho-p44/42 MAPK (Thr202/Tyr204) antibody, rabbit polyclonal p44/42 MAPK antibody, rabbit polyclonal phospho-Akt (Ser473) antibody, and rabbit polyclonal Akt antibody (all from Cell Signaling Technology, Beverly, MA); and mouse monoclonal anti-phospho-EGFR (Y1173) antibody and mouse monoclonal anti-EGFR (non-phospho-Y1173) antibody (from Upstate Biotechnology, Lake Placid, NY). For immunohistochemical studies, the primary antibodies used were mouse monoclonal clone 74 anti-phospho-EGFR (from Chemicon, Temecula, CA), mouse monoclonal Ki67 antibody clone MIB-1, mouse monoclonal anti-EGFR antibody clone 2--18C9, and mouse monoclonal anti-CD34 antibody clone QBEnd 10 (from DakoCytomation, Carpinteria, CA). The primary antibodies for phospho-MAPK and phospho-Akt were the same used for Western blot assays.

Cell Lines. Vulvar squamous carcinoma cells [A431(13)], colon carcinoma cells [DiFi (14)], prostate carcinoma cells [DU145 (15)], and breast carcinoma cells [SK-BR-3 (13)], MDA-MB-435S (16), MDA-MB-468 (17), MDA-MB-453 (18), T-47D (16), and BT-474 (10)] were obtained from the American Type Culture Collection (Manassas, VA). Cell lines were maintained as monolayers at 37°C and 5% CO_2/air in DMEM/Ham's F-12 supplemented with 10% fetal bovine serum and glutamine (2 mmol/L); and, in the case of BT-474 and MDA-MB-435S, insulin at 0.01 μg/mL was added.

Growth Assays. Cells were seeded into six-well culture plates at 10^5 cells per well. After attachment (24 hours), cells were exposed to different concentrations of gefitinib (0.1, 1, and 10 μmol/L) and/or cetuximab (0.5, 5, and 50 nmol/L) for 72 hours. After drug incubation, cells were washed once with PBS, harvested in 0.1% trypsin-1 mmol/L EDTA in PBS, and counted with a Coulter counter.

Western Blot Analyses. Western blot assays were performed as previously reported (19) with minor modifications. In brief, A431 tumor cells were grown in 100-mm dishes until subconfluence and then exposed to gefitinib (0.1 and 1 μmol/L) and/or cetuximab (0.5 and 5 nmol/L) for 2 hours. After removal of media, cells were washed twice with ice-cold PBS and scraped into ice-cold lysis buffer [50 mmol/L HEPES (pH 7.0), 10% glycerol, 1% Triton X-100, 5 mmol/L EDTA, 1 mmol/L $MgCl_2$, 25 mmol/L NaF, 50 μg/mL leupeptin, 50 μg/mL aprotinin, 0.5 mmol/L orthovanadate, and 1 mmol/L phenylmethylsulfonyl fluoride]. After removal of cell debris by centrifugation, protein concentration was determined by Lowry assay (DC Protein assay, Bio-Rad, Hercules, CA). Lysate samples containing equal amounts of protein were then added to SDS-PAGE loading buffer with 5% β-mercaptoethanol and heated 5 minutes at 100°C. Electrophoretic transfer to nitrocellulose membranes was followed by immunoblotting with the primary antibodies described in the "Compounds" section. Finally, membranes were hybridized with the appropriate horseradish peroxidase-conjugated secondary antibody (Amersham Pharmacia Biotech, Little Chalfont, United Kingdom) and were detected via chemiluminescence with the SuperSignal West Dura Extended Duration Substrate (Pierce, Rockford, IL).

RNA Extraction, Probe Synthesis, and Hybridization on cDNA Arrays. Total RNA was isolated from A431 untreated cells (controls, $n = 2$) and cells treated with gefitinib (0.1 and 1 μmol/L) or cetuximab (0.5 and 5 nmol/L) for 24 hours ($n = 4$). Total RNA was isolated with TRIZOL reagent (Life Technologies, Inc., Gaithersburg, MD) as indicated by the manufacturer. Purity of isolated RNA was evaluated spectrophotometrically by the A260-to-A280 absorbance ratio. Three micrograms of total RNA from endometrial samples and Universal Human Reference RNA (Stratagene) were used as control, and T7-$(deoxythymidine)_{24}$ oligonucleotide primers were used to amplify the double-strand cDNA synthesis by the Superscript Choice System (Life Technologies, Inc., Gaithersburg, MD). *In vitro* transcription was carried out with Megascript T7 (Ambion, Austin, TX). Amplified RNA was obtained and purified with TRIZOL reagent, and the integrity was measured spectrophotometrically by the A260-to-A280 ratio or by gel electrophoresis. Three micrograms of amplified RNA was used to generate fluorescence cDNA by transcriptional synthesis with Superscript enzyme protocol (Life Technologies, Inc.). In a set of hybridizations ($n = 6$), all of the cell samples were labeled with Cy5-dUTP fluorochrome (Amersham, Uppsala, Sweden) and the reference pool with Cy3-dUTP fluorochrome (Amersham), as described previously (20, 21). An additional set of hybridizations ($n = 6$) was carried out after labeling the samples and pool with the reverse fluorochrome (Cy3-dUTP for the samples and Cy5-dUTP for the pool).

Hybridization was performed in 4× standard saline citrate, 1× bovine serum albumin, 2 μg/mL DNAs, and 0.1% SDS at 42°C for 15 hours. Slides were washed, dried, and then scanned in a Scanarray 5000 XL scanner (GSI Lumonics Kanata, Ontario, Canada) at wavelengths of 635 and 532 nm for Cy5 and Cy3 dyes, respectively, to obtain 10-μm resolution images, which were quantified with the GenePix Pro 4.0 program (Axon Instruments Inc., Union City, CA).

The cDNA array chip is a new version of the CNIO Oncochip (22) manufactured by the CNIO Genomic Unit (http://bioinfo.cnio.es/data/oncochip).[5] This version contains 9,726 clones corresponding to 6,386 different genes. The chip includes 2,489 clones that have been printed in duplicate to assess reproducibility.

Data Analysis. Fluorescence intensity measurements from each array element were compared with the median of local background in each channel, and the elements with values less than this median were excluded. In addition, all spots smaller than 25 μm were manually deleted. After applying these filters, a total of 5,345 spots were evaluated. The expression ratios of the duplicated spots on the array were averaged. The final expression ratio for each gene in treated cells was obtained after dividing its value into that obtained in untreated control cells.

To find a set of genes that were differentially expressed in cells treated with different compounds (gefitinib and cetuximab), we used a *t* test after 10,000 permutations. We considered genes to be differentially expressed if they had an unadjusted *P* value of ≤0.03. Statistical comparison was performed with the POMELO (CNIO, Madrid, Spain) program.[6]

Validation data. Semiquantitative reverse transcription-PCR and quantitative real-time PCR (TaqMan) were carried out to validate data of cDNA microarrays of selected genes.

Semiquantitative reverse transcription-PCR was performed with Superscript II system for reverse transcription beginning with 0.5 μg of total RNA and random primers in a 20-L reaction volume. cDNA product and 0.4 to 1 μg oligonucleotide were heated at 95°C for 5 minutes, followed by 30 cycles of PCR amplification: 94°C denaturing during 1 minute, 55°C to 58°C annealing for 1 minute, and 72°C extension for 1 minute, followed for 10 minutes at 72°C as final extension. Primers sequences were designed with a OLIGO 4.0 program for the amplification of selected sequences of the following genes: *PI3KCD*, Forward (F), 5′-GCCTTCCCCAGACAGAAACA-3′, and Reverse (R), 5′-GGAGCACACTTTGCAAAGCC-3′; *PLAU* (F), 5′-GGACTGAAGCCTGCAGGAGT-3′, and (R), 5′-CCTATAACCTCTCCCAGAAAGA-3′; *EMS1* (F), 5′-GCAGTTTCCACACGGGCTGTCC-3′, and (R), 5′-GCAGGCCACGCTGTGTCCATC-3′; *CDH1* (F), 5′-GACGCGGACGATGATGTGAAC-3′, and (R) 5′-TTGTACGTGGTGGGATTGAAGA-3′; and *GAPDH* (F), 5′-TGGTATCGTGGAAGGACTCATGAC-3′, and (R), 5′-ATGCCAGTGAGCTTC CCGTTCAGC-3′. PCR products were visualized on 3% agarose gels stained with ethidium bromide, and images were captured and quantified by Quantity One (Bio-Rad, Hercules, CA).

Quantitative real-time PCR (TaqMan) was performed as previously reported (22). As internal standard, we used β2-microglobuline (Applied Biosystems, Foster City, CA). The sequence of oligonucleotides and TaqMan probes used for the analysis of *TRAIL* were obtained with the Assays-by-Design (SM) File Builder program (Applied Biosystems).

A431 Xenografts in Nude Mice. All of the experimental procedures were approved, and mice were maintained and treated in accordance with institutional guidelines of Vall d'Hebron University Hospital Animal Care and Use Committee. Six-to-eight-week-old female BALB/c athymic (*nu*+/*nu*+) mice were purchased from Charles River Laboratories (Paris, France). The initial body weight of the animals at the time of arrival was between 18 and 20 g. Mice were allowed to acclimatize to local conditions for 1 week before receiving injections of cancer cells. Mice were housed in air-filtered laminar flow cabinets and handled with aseptic procedures with a 12-hour light cycle and food and water *ad libitum*. Logarithmically growing A431 cells were harvested by trypsinization, and each mouse was given injections of 1×10^6 cells subcutaneously into the right flank

In these experiments, tumors were allowed to reach a predetermined size before the start of treatment with vehicle (control), gefitinib, cetuximab or a combination of both at the dose and schedule described. Animals in the control group were treated with an orally given vehicle (0.05% Tween/d by mouth) and sterile PBS given by intraperitoneal injection twice a week. Gefitinib was diluted in 0.05% Tween.

[5] Internet address: http://bioinfo.cnio.es/data/oncochip.

[6] Internet address: http://pomelo.bioinfo.cnio.es/.

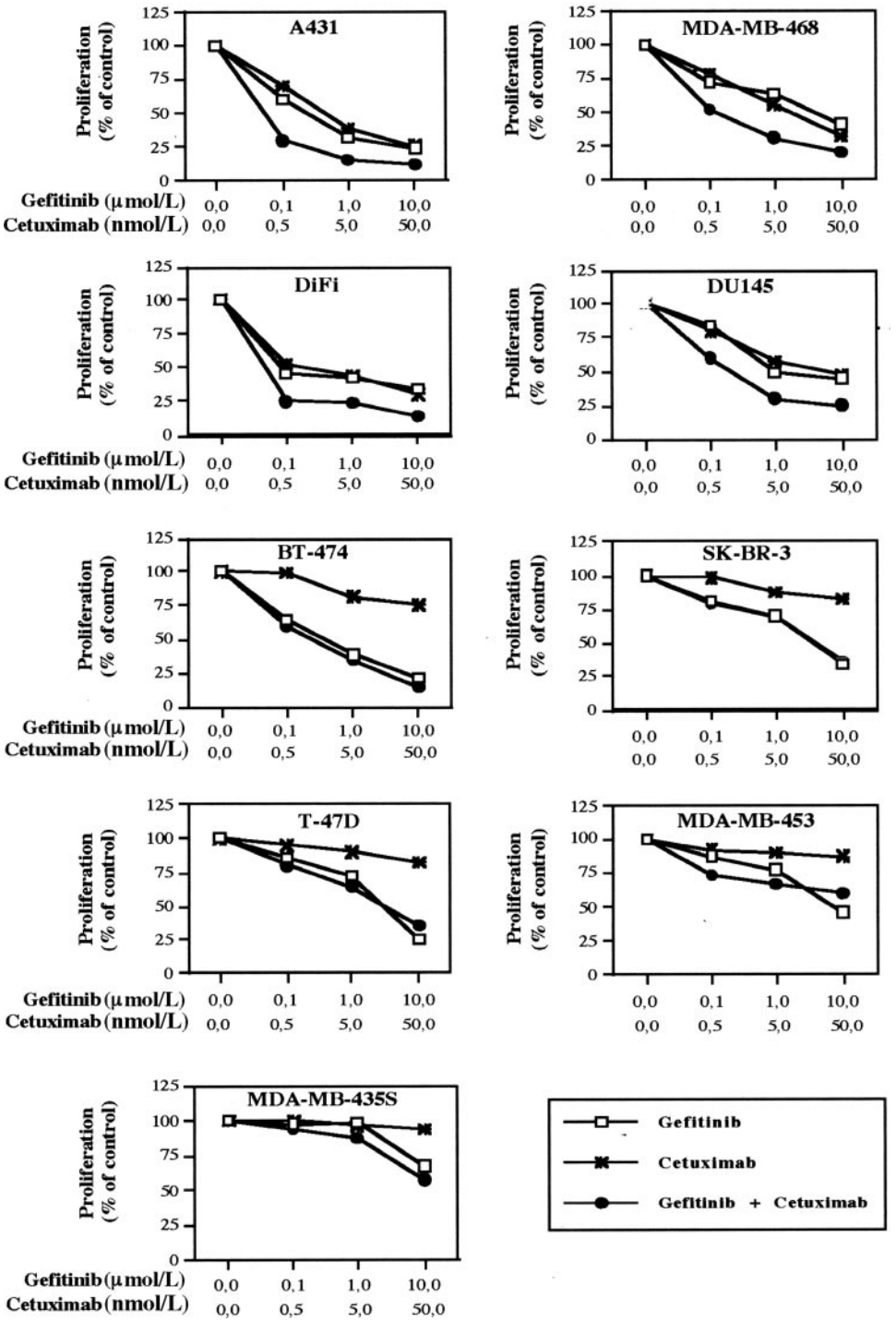

Fig. 1 Dose-dependent growth-inhibitory effect of gefitinib and cetuximab as single agents or in combination in a panel of human cancer cell lines with different levels of EGFR and HER2 expression (EGFR high/HER2 low: A431, MDA-MB-468, DiFi, DU145; EGFR low/HER2 high: BT-474, SK-BR-3, T-47D, MDA-MB-453; EGFR low/HER2 low: MDA-MB-435S). Cells were plated in six-well dishes and were treated the next day with increasing doses of gefitinib, cetuximab, or the combination for 72 hours. Results are expressed as percentage of cell number compared with the same cell line grown in the absence of the drugs. The data shown represent the median values of triplicate experiments.

Tumor growth was assessed twice weekly by caliper measurement. Tumor volume (mm^3) was calculated by the formula $\pi/6 \times$ larger diameter $\times$ (smaller diameter)^2 Results are presented as mean $\pm$ SEM. Student's *t* test was used to compare tumor sizes among different groups at the end of treatment. In the study design I and II, all of the mice were sacrificed at the end of treatment, and their tumors were harvested for immunohistochemical analysis, except for tumor-free mice, which continued to be monitored for an additional 8 months. In the study design III, mice were followed until tumors grew to a size mandating sacrifice.

Immunohistochemistry. For immunohistochemical analysis, excised tumors were fixed immediately in 10% buffered neutral formalin for 18 hours, and then were dehydrated and

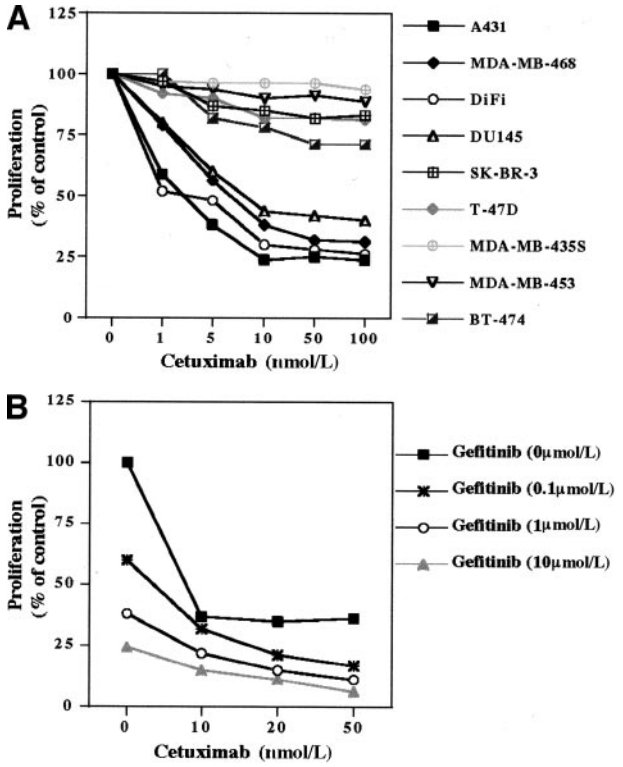

Fig. 2 *A*, dose-dependent growth-inhibitory effect of cetuximab in a panel of human cancer cell lines. Results are expressed as percentage of cell number compared with the same cell line grown in absence of the drug. A maximal growth-inhibitory effect is reached at a concentration close to 10 nmol/L. In *B*, in A431 cells, the addition of gefitinib to maximally growth-inhibitory doses of cetuximab results in additional growth inhibition. The data shown represent the median values of triplicate experiments.

paraffin embedded. Immunostaining was performed with 4-μm tissue sections placed on plus-charged glass slides. After deparaffinization in xylene and graded alcohols, endogenous peroxidase was blocked by immersing the sections in 0.03% hydrogen peroxide for 5 minutes. Slides were washed for 5 minutes with Tris-buffered saline solution containing Tween 20 at pH 7.6 and incubated with the same primary antibodies used for Western blotting, followed by incubation with a specific anti-immunoglobulin horseradish peroxidase-conjugated to detect antigen–antibody reaction (DakoCytomation, Carpinteria, CA). Sections were then visualized with 3,3′-diaminobenzidine as a chromogen for 5 minutes and were counterstained with hematoxylin. Slides were washed in tap water, dehydrated, and mounted with glass coverslips. All of the immunohistochemical stainings were performed in a Dako Autostainer, and the same sections incubated with nonimmunized serum were used as negative controls. As positive control, sections of a head and neck human tumor with a known expression of the markers were stained. The percentage of stained tumor cells was scored from these sections in 10 high-power optical microscopic fields (×400) in a blinded fashion, and the average percentage of tumor cell staining for each antibody was calculated. Grading of positivity ranged from a score of 1% to 100%. This scoring was used for statistical analysis.

Apoptosis Assay. To evaluate treatment-induced apoptosis, we plated 3×10^6 A431 cells in complete medium in 150-mm tissue culture dishes and incubated them with different concentrations of gefitinib and/or cetuximab. After 3 days, both adherent and detached cells were harvested. Then, cells were centrifuged at 1000 rpm and were fixed in 10% buffered neutral formalin, dehydrated, and paraffin embedded. Additionally, apoptosis was determined in the resected tumors. terminal deoxynucleotidyl transferase (TdT)-mediated dUTP nick end labeling (TUNEL) was performed on 4-μm sections from cell and tissue blocks. Slides were deparaffined and rehydrated through graded alcohols to water, were digested with proteinase-K (20 μg/mL) for 10 minutes, were washed in PBS, and were incubated with equilibration buffer (TdT buffer) for 15 minutes, followed by incorporation of 16-dUTP-fluorescein (Roche Diagnostics Gmbh, Mannheim, Germany) in the presence of working-strength TdT for 90 minutes at 37°C. Distilled water instead of TdT was used for negative controls. Stop-wash TB solution was used for 15 minutes to stop the reaction, whereafter the sections were washed in PBS, and nuclei were stained with 0.1 μg/mL 4′-diamidino-2-phenylindone (DAPI) for 5 minutes. Slides were viewed with a fluorescence microscope (Nikon E400, Tokyo, Japan), and apoptotic cells were quantified and

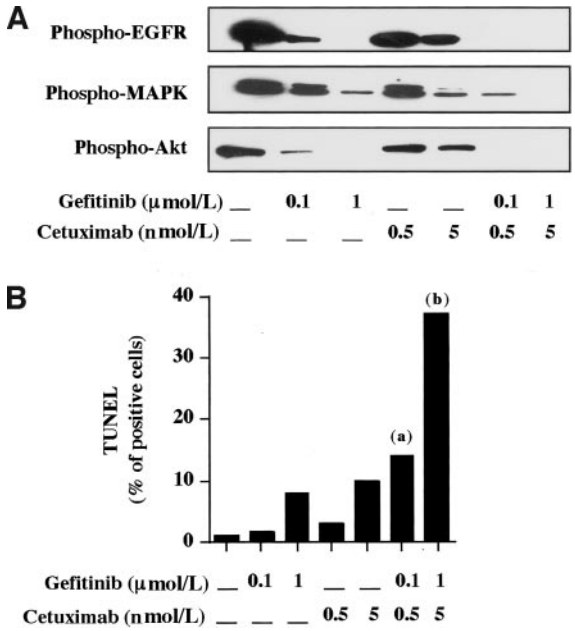

Fig. 3 *A*, Western blot analysis for phosphorylated EGFR, MAPK, and Akt in A431 cells exposed to different concentrations of gefitinib and cetuximab alone and in combination. Cells were grown in 100-mm dishes until subconfluence and then were exposed to gefitinib, cetuximab, and the combined treatment with the two agents for 2 hours. *B*, induction of apoptosis by treatment with gefitinib, cetuximab, or the combination in A431 cells. Analysis of apoptosis was performed by TUNEL assay, as described in Materials and Methods. Data represent the median values of triplicate experiments. Apoptotic cells are expressed as percentage of total number cells (×400). Mann–Whitney *U* test: *(a)*, gefitinib 0.1 μmol/L + cetuximab 0.5 nmol/L *versus* gefitinib 0.1 μmol/L and *versus* cetuximab 0.5 nmol/L: $P < 0.05$; *(b)*, gefitinib 1 μmol/L + cetuximab 5 nmol/L *versus* gefitinib 1 μmol/L and *versus* cetuximab 5 nmol/L: $P < 0.05$.

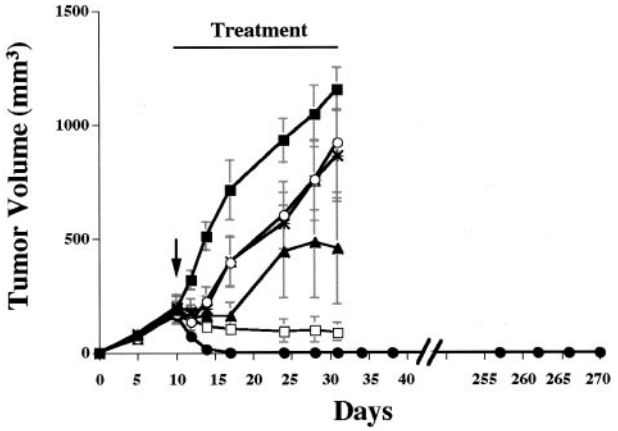

Fig. 4 Antitumor activity of gefitinib, cetuximab and gefitinib + cetuximab in A431 human tumor xenografts (study design I). Tumors were allowed to reach 200 mm^3 before treatment was started (day 10) and animals were divided into groups of 10 animals each. ■, control; ○, gefitinib, 25 mg/kg/d; ▲, gefitinib, 50 mg/kg/d; *, cetuximab, 1 mg twice a week; □ gefitinib (25 mg/kg/day) + cetuximab (1 mg twice a week); ●, gefitinib (50 mg/kg/d) + cetuximab (1 mg twice a week). Animals were treated for 3 weeks and were then sacrificed on day 31 with the exception of tumor-free animals, which were monitored for tumor recurrence. Data are expressed as mean (*bars*, SEM) tumor volume. Student's *t* test was used to compare tumor sizes among different groups at the end of treatment. Gefitinib (25 or 50 mg/kg) and cetuximab 1 mg, *versus* control (no significant for all comparisons); gefitinib 25 mg/kg + cetuximab 1 mg, *versus* gefitinib 25 mg/kg ($P < 0.01$); gefitinib 25 mg/kg + cetuximab 1 mg, *versus* cetuximab 1 mg ($P < 0.01$); gefitinib 50 mg/kg + cetuximab 1 mg, *versus* gefitinib 50 mg/kg ($P < 0.001$); gefitinib 50 mg/kg + cetuximab 1 mg, *versus* cetuximab 1 mg ($P < 0.001$).

expressed as percentage of total number of cells, in 10 random fields at ×400.

Tumor Vascular Density. Intratumoral microvessels were stained with an anti-CD34 antibody by immunohistochemistry. The Chalkley counting method was applied for estimating the vascular density in the tumors. A 25-random-point Chalkley reticule (Chalkley grid area 0.196 mm^2, Olympus, Tokyo, Japan) was used in an optical microscope at ×250, and the dots on or within the vessels in the stroma of tumors were counted. Five microscopic fields were evaluated in each tumor, and the mean value was calculated.

Analysis of Combination Effect. *In vitro* drug interactions were analyzed according to Chou and Talalay (23) with the Calcusyn program (Biosoft, Cambridge, United Kingdom). This software calculates the median effect dose, D_m, (analogous to the IC_{50}) of the drug combinations with the median effect equation. Determination of synergy or antagonism was quantified by the combination index (*CI*). $CI = 1$ indicates an additive effect, *CI* of <1 indicates synergy, and *CI* of >1 indicates antagonism. *In vivo* combination analysis was performed by the fractional product method (24). According to this method, the effects of two or more drugs, when combined, can be calculated by multiplying the fractional tumor volume by each single drug. If the effect of the drugs acting simultaneously is equal to, larger than, or smaller than that calculated, it has been assumed that additivity, synergism, or antagonism, respectively, has occurred.

RESULTS

***In vitro* Effects of the Combined Treatment with Gefitinib and Cetuximab on a Panel of Cancer Cell Lines.** We evaluated the *in vitro* antiproliferative activity of gefitinib and cetuximab given alone or in combination on a panel of human cancer cell lines with different expression of EGFR and HER2. For this purpose, we selected tumor cell lines that we had previously determined to have medium-to-high EGFR and low HER2 levels, such as A431, MDA-MB-468, DiFi, and DU145 cells; tumor cell lines with high HER2 and low EGFR levels, such as BT-474, SK-BR-3, MDA-MB-453 and T-47D cells (7); the MDA-MB-435S cells, which are known to express very low or undetectable levels of both receptors, were included in the assays (7–9).

The growth-inhibitory effects of single-agent gefitinib and cetuximab are shown in Fig. 1. In summary, cetuximab markedly inhibited the proliferation of cell lines with medium-to-high levels of EGFR (A431, MDA-MB-468, DiFi, and DU145), but did not inhibit the growth of cell lines with low level of EGFR expression. As expected, gefitinib, in addition to inhibiting the growth of cells with elevated EGFR expression, inhibited also the proliferation of cell lines with high levels of HER2 (BT-474 and SK-BR-3 cells) or with an active HER2 pathway (MDA-MB-453 cells; refs. 7–9, 18). Gefitinib and cetuximab did not inhibit growth of MDA-MB-435S cells, which express very minimal or no EGFR levels.

To evaluate the nature of the interaction between gefitinib and cetuximab (additive or synergistic), combination analyses were performed with the Combination Index (*CI*) method (23). Using fixed doses of gefitinib and cetuximab, we assessed the effects of the combination in our panel of cancer cells (Fig. 1). *CI* values for the combination treatment with gefitinib and cetuximab were <1 (synergism) for all cell lines with medium-to-high level of EGFR-expression (A431, MDA-MB-468, DiFi, and DU145). In contrast, no cooperative effects between gefitinib and cetuximab were observed in tumor cell lines expressing low or undetectable EGFR levels, regardless of their HER2 status (BT-474, SK-BR-3, T-47D, MDA-MB-453, and MDA-MB-435S).

To further confirm the superiority of combined treatment over single-drug exposure, we planned experiments with the maximally effective dose of cetuximab, given alone or in combination with gefitinib. As shown in Fig. 2*A*, the antiproliferative effect of cetuximab on tumor cell lines that are growth inhibited by the monoclonal antibody is dose dependent until a concentration of 10 nmol/L is reached; higher doses do not further inhibit growth (plateau effect). In a subsequent experiment, A431 cells were exposed to different concentrations of gefitinib (0.1, 1, and 10 μmol/L), in combination with cetuximab at plateau doses (10, 20, and 50 nmol/L). An additive growth-inhibitory effect was found for each treatment point (Fig. 2*B*). Therefore, gefitinib in a situation of maximal growth inhibition by cetuximab results in an additional dose-dependent inhibition of cell growth. The converse could not be studied because gefitinib does not have a plateau effect, probably because of nonspecific kinase inhibition at higher doses.

Table 1 Antitumor activity of gefitinib and cetuximab, given alone or in combination against A431 tumors xenografted in nude mice

Study design	Treatment		Tumor-growth inhibition (% of control)*	Tumor-free mice (no. of remissions/total)†	Body weight (mean g ± SEM)‡
	Compound	Dose			
I	—	—	—	0/10	19.1 ± 1.7
	gefitinib	25 mg/kg	20	0/10	20.6 ± 0.2
	gefitinib	50 mg/kg	61	0/10	20.2 ± 0.4
	cetuximab	1 mg/mouse	25	0/10	21.1 ± 0.3
	gefitinib + cetuximab	25 mg/kg + 1 mg/mouse	92	3/10	20.6 ± 0.4
	gefitinib + cetuximab	50 mg/kg + 1 mg/mouse	100	10/10	19.0 ± 0.3
II	—	—	—	0/12	23.2 ± 0.5
	gefitinib	50 mg/kg	12	0/12	20.7 ± 0.6
	gefitinib	100 mg/kg	37	0/12	20.4 ± 0.8
	cetuximab	1 mg/mouse	31	0/12	22.4 ± 0.5
	cetuximab	1.5 mg/mouse	64	0/12	22.3 ± 0.6
	gefitinib + cetuximab	50 mg/kg + 1.5 mg/mouse	99	11/12	19.7 ± 0.5
	gefitinib + cetuximab	100 mg/kg + 1.5 mg/mouse	100	12/12	19.0 ± 0.4
III	—	—	—	0/10	22.0 ± 0.8
	gefitinib	50 mg/kg	77	0/10	20.0 ± 0.6
	gefitinib	200 mg/kg	100	10/10	18.0 ± 0.6
	cetuximab	1 mg/mouse	31	2/10	21.9 ± 0.5
	cetuximab	1.5 mg/mouse	87	6/10	21.2 ± 0.4
	gefitinib + cetuximab	50 mg/kg + 1 mg/mouse	100	10/10	20.3 ± 0.3

Note. Study design I and III treatment was initiated when tumors were ~200 mm^3 in size; study design II treatment was initiated when tumors were ~500 mm^3 in size.

* Percentage of tumor growth inhibition relative to control, at the end of the treatment (study design I, day 31; study design II, day 36; study design III, day 34).

† Tumor-free animals/total number of animals, at the end of the treatment.

‡ Body weight at the end of the treatment.

Effects of Gefitinib and Cetuximab on EGFR Signaling Pathways and Apoptosis. We assessed the effects of gefitinib and cetuximab on phosphorylation of EGFR, MAPK, and Akt, in A431 cells (Fig. 3*A*). The doses of gefitinib and cetuximab that caused a decline in cell proliferation were the same that reduced EGFR, MAPK, and Akt activation (phosphorylation), according to Western blot analysis. A more pronounced decrease in the levels of phosphorylation of each marker was observed after combined treatment with gefitinib and cetuximab, as compared with treatment with each single drug, at two different dose combinations [gefitinib (μmol/L)/cetuximab (nmol/L): 0.1/0.5 and 1/5]. This short-time treatment (2-hour) with gefitinib and cetuximab did not produce any significant changes in the endogenous levels of EGFR, MAPK, or Akt (data not shown).

We determined next whether the combined treatment could enhance the apoptotic effect of each drug given separately (Fig. 3*B*). The percentage of apoptotic cells was determined on day 3 from the beginning of treatment with gefitinib and/or cetuximab. Both agents alone induced apoptotic cell death in a dose-dependent manner. However, treatment with the combination resulted in greater induction of apoptosis when compared to either of the agents given alone. The lower dose combination, 0.1 μmol/L gefitinib plus 0.5 nmol/L cetuximab, induced apoptosis in 14% of cells, whereas the same doses of gefitinib and cetuximab given alone resulted in apoptosis in only 1.5 and 3% of cells, respectively. Likewise, at the higher dose level (1 μmol/L gefitinib plus 5 nmol/L cetuximab) the apoptotic rate was 37%, clearly superior to the 8 and 10% of apoptosis with single-agent gefitinib and cetuximab, respectively.

***In vivo* Studies of the Combination of Gefitinib and Cetuximab in A431 Human Tumor Xenografts in Nude Mice.** To characterize the *in vivo* effects of the combination, we conducted a series of experiments in A431 human tumor xenografts, a cell line that expresses high levels of EGFR.

In the study design I, we used single-agent doses of gefitinib (25 and 50 mg/kg/d) and cetuximab (1 mg per mouse, twice a week) that only partially inhibit tumor growth without inducing any complete tumor remission (Fig. 4). In contrast, the combination of gefitinib (25 mg/kg) + cetuximab resulted in a 92% growth inhibition and induced complete remission in 3 of 10 animals, whereas regression of established A431 tumors was observed in 100% (10 of 10) of animals treated with the combination of gefitinib (50 mg/kg) + cetuximab (Table 1). In this

Table 2 Study design I. Fractional tumor volume (FTV) relative to untreated controls for gefitinib, cetuximab and combination treatment (expected vs. observed)

Day*	Gefitinib (25 mg/kg)	Cetuximab (1 mg/mouse)	Expected†	Observed	*R*‡
7	0.555	0.559	0.310	0.140	2.2
14	0.647	0.610	0.395	0.100	3.9
21	0.798	0.750	0.599	0.077	7.8

Note. FTV = (mean tumor volume experimental)/(mean tumor volume control).

* Day after start of treatment.

† (Mean FTV of gefitinib) × (mean FTV of cetuximab).

‡ Obtained by dividing the expected FTV by the observed FTV. A ratio of >1 indicates a synergistic effect, and a ratio of <1 indicates a less than additive effect.

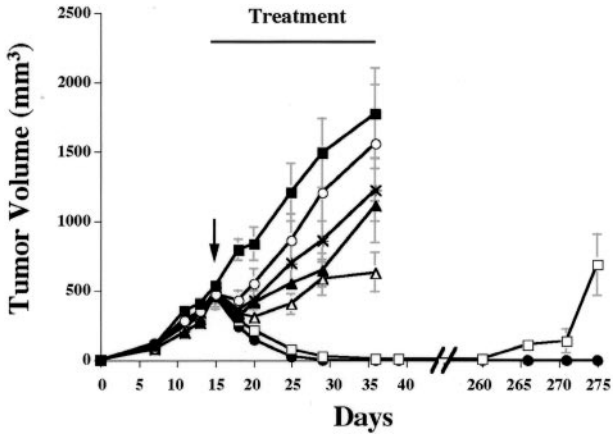

Fig. 5 Antitumor activity of gefitinib, cetuximab, and the combination in A431 human tumor xenografts (study design II). When tumors reached 500 mm^3 in size, the mice were divided in groups of 12 animals each and treatment was started. ■, control; ○, gefitinib, 50 mg/kg/d; ▲, gefitinib, 100 mg/kg/d; *, cetuximab, 1 mg twice a week; △, cetuximab, 1.5 mg twice a week; □, gefitinib(50 mg/kg/d) + cetuximab (1.5 mg twice a week); ●, gefitinib (100 mg/kg/d) + cetuximab (1.5 mg twice a week). Animals were treated for 3 weeks and were then sacrificed on day 36 with the exception of tumor-free animals that were monitored for tumor recurrence. Data are expressed as mean (*bars*, SEM) tumor volume. Student's *t* test was used to compare tumor sizes among different groups at the end of treatment. Gefitinib (50 or 100 mg/kg) and cetuximab, 1 mg, *versus* control ($P > 0.05$ for all comparisons); cetuximab, 1.5 mg, *versus* control ($P < 0.01$); gefitinib 50 mg/kg + cetuximab 1.5 mg, *versus* gefitinib 50 mg/kg ($P < 0.001$); gefitinib 50 mg/kg + cetuximab 1.5 mg, *versus* cetuximab 1.5 mg ($P < 0.001$); gefitinib 100 mg/kg + cetuximab 1.5 mg, *versus* gefitinib 100 mg/kg ($P < 0.001$); gefitinib 100 mg/kg + cetuximab 1.5 mg, *versus* cetuximab 1.5 mg ($P < 0.001$).

Table 3 Study design II. Fractional tumor volume (FTV) relative to untreated controls for gefitinib, cetuximab and combination treatment (expected vs. observed)

Day*	Gefitinib (50 mg/kg)	Cetuximab (1.5 mg/mouse)	Expected†	Observed	*R*‡
7	0.712	0.335	0.239	0.067	3.6
14	0.809	0.395	0.320	0.018	17.8
21	0.878	0.357	0.313	0.006	52.2

Note. FTV = (mean tumor volume experimental)/(mean tumor volume control).

* Day after start of treatment.

† (Mean FTV of gefitinib) × (mean FTV of cetuximab).

‡ Obtained by dividing the expected FTV by the observed FTV. A ratio of >1 indicates a synergistic effect, and a ratio of <1 indicates a less than additive effect.

latter group, no tumors regrew after 8 months from the completion of therapy. All of the treatments were well tolerated, and there were no signs of toxicity or body weight loss during therapy. Analysis of the *in vivo* interaction between both drugs was performed by the fractional product method. Table 2 summarizes relative tumor volume of treated groups on three different time points in this experimental design (I). Combination therapy with gefitinib (25 mg/kg) and cetuximab (1 mg per mouse) showed a synergistic effect on tumor-growth inhibition at the various analyzed time points. On day 7, there was a 2.2-fold improvement in antitumor activity in the combination group when compared with the expected additive effect. On day 21, the gefitinib and cetuximab combination group showed a 7.8-fold higher inhibition of tumor growth over an additive effect (expected fractional tumor volume). Similar results were obtained with combination therapy with gefitinib (50 mg/kg) and cetuximab (1 mg per mouse; data not shown).

In the study design II, a more stringent test for the combination was provided because a larger tumor burden was allowed to develop before treatment start (tumor size ~500 mm^3; Fig. 5). In this setting of greater initial tumor burden, equal or higher doses of gefitinib (50 or 100 mg/kg), and cetuximab (1 or 1.5 mg per mouse) than in study design I resulted in only a partial inhibition of tumor growth. On the other hand, combination therapy with cetuximab and gefitinib resulted in a significant inhibition of tumor growth compared with cetuximab or gefitinib given alone ($P < 0.001$). Complete regression of these large tumors was observed in the combination group in almost all (11 of 12) of the tumors treated with gefitinib 50 mg/kg and in all (12 of 12) of the tumors treated with gefitinib 100 mg/kg (Table 1). At the end of treatment, tumor-free mice belonging to the groups treated with combination therapy were monitored for an additional 8 months. Some tumors (7 of 11) in the group treated with the lowest dose of gefitinib (50 mg/kg) plus cetuximab resumed growth in this follow-up period. However, all of the mice (12 of 12) in the higher-dose combination group remained in complete remission for the duration of the follow-up period. Table 3 shows the analysis of the enhanced combination effect at different time points during therapy in the

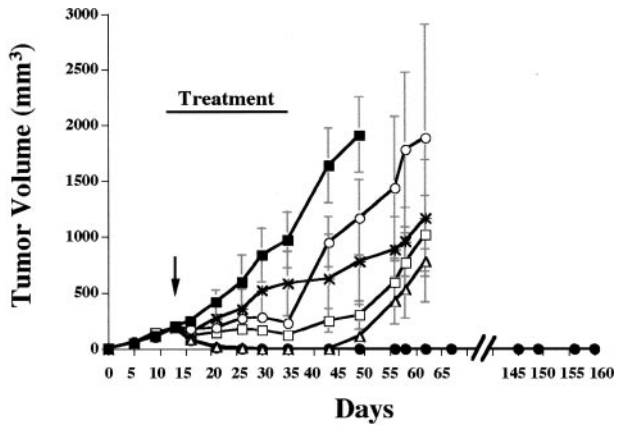

Fig. 6 Antitumor activity of gefitinib, cetuximab, and the combination in A431 human tumor xenografts (study design III). When tumors reached 200 mm^3 in size (day 13) they were divided into groups of 10 animals each and treatment was started. ■, control; ○, gefitinib, 50 mg/kg/d; △, gefitinib, 200 mg/kg/d; *, cetuximab, 1 mg twice a week; □, cetuximab, 1.5 mg twice a week; ●, gefitinib (50 mg/kg/d) + cetuximab (1 mg twice a week). Animals were treated for 3 weeks. Data are expressed as mean (*bars*, SEM) tumor volume. Student's *t* test was used to compare tumor sizes among different experimental groups. At the end of treatment (day 34): gefitinib 50 mg/kg + cetuximab 1 mg, *versus* gefitinib 200 mg/kg or cetuximab 1.5 mg ($P > 0.05$). Twenty-eight days after treatment withdrawal (day 62): gefitinib 50 mg/kg + cetuximab 1 mg, *versus* gefitinib 200 mg/kg or cetuximab 1.5 mg ($P < 0.01$).

Table 4 Immunohistochemical analysis of A431 xenografts

Groups	Control*	Gefitinib (25 mg/kg)*	Gefitinib (50 mg/kg)*	Cetuximab (1 mg/mouse)*	Gefitinib (25 mg/kg) + cetuximab (1 mg/mouse)*	Gefitinib (50 mg/kg) + cetuximab (1 mg/mouse)*
pEGFR	52	35	25	32	13†	2†
pMAPK	37	25	10	24	13†	5†
pAkt	34	24	47	48	6†	0†

* Mean of percentage of tumor cell staining for each antibody.
† $P < 0.01$ (Mann–Whitney U test).

experimental design II. The indices (R) for combination therapy with gefitinib (50 mg/kg) and cetuximab (1.5 mg) were >1, indicating a synergistic interaction between the drugs. Similar findings were observed for combination therapy with gefitinib (100 mg/kg) and cetuximab (1.5 mg; data not shown).

In the study design III, the objective was to compare whether high single-agent doses of gefitinib and cetuximab could prove equivalent to lower doses of both agents given in combination (Fig. 6). In the case of gefitinib, the chosen dose was 200 mg/kg/d, the highest published dose that had been used in xenograft models and that had been reported to induce complete, but transient, tumor regressions (25). The chosen high dose for cetuximab was 1.5 mg per mouse twice a week, which was 50% higher than the highest published dose in xenograft models (26) High-dose single-agent cetuximab and gefitinib were able to induce complete tumor regressions in 6 of 10 and 10 of 10 animals, respectively (Table 1). However, in concordance with prior studies (25, 26), all of the tumors resumed growing when treatment was discontinued. In contrast, the combination of lower doses of gefitinib and cetuximab (50 mg/kg and 1 mg, respectively) resulted in a complete regression of tumors in all mice (Table 1). Furthermore, all of the animals in this group remain tumor free at 4 months of follow-up.

Immunohistochemical Analysis. An immunohistochemical analysis of A431 tumors excised at the end of treatment in the experimental design I was performed. Because a 100% of tumor growth inhibition was observed in tumor-bearing mice treated with the combination of gefitinib (50 mg/kg) and cetuximab (1 mg per mouse), a satellite group treated with this combination was included to obtain tumor samples for immunohistochemical analysis. Mice from this satellite group were sacrificed 5 days after treatment start (90% of tumor-growth inhibition with respect to untreated control group), and their tumors were taken for analysis.

The results showed a significant decrease of pEGFR, pMAPK, and pAkt in tumor samples belonging to the combination groups compared with each single-drug therapy and control group ($P < 0.01$; Table 4; Fig. 7*A*). Moreover, a reduction in tumor cell proliferation (Ki67) and tumor vascularization (CD34), and an increase in tumor cell apoptosis (TUNEL) were observed in tumors treated with the combination of gefitinib and cetuximab (Fig. 7*B*). The combined treatment resulted in a >36-fold decrease in tumor cell proliferation, a >3.5-fold decrease in vessel staining, and >2.7-fold increase in tumor cell apoptosis, compared with either agent alone or control group ($P < 0.01$ for all comparisons).

Microarray Analysis. To obtain comprehensive gene expression profiles modified by gefitinib or cetuximab treatment of A431 cells, we used cDNA microarray to investigate 6,386 genes represented by 9,726 clones. To evaluate the genes modified by gefitinib or cetuximab in a dose-independent manner, we calculated the average expression value of each gene for both doses of gefitinib (0.1 and 1 μmol/L) and cetuximab (0.5 and 5 nmol/L).

After array processing, the genes were classified as commonly changed after treatment with gefitinib and cetuximab if their ratio were ≥2-fold up- or down-regulated with respect to untreated cells. By this criterion, there were 20 genes commonly up-regulated and 39 down-regulated genes (Table 5). We found that six genes involved in cell cycle control and DNA replication (*cyclin H, C,* and *A*, *primase*, and *topoisomerase I* and *II*) were similarly down-regulated by gefitinib and cetuximab. In addition, the expression of several molecules involved in cell adhesion control was affected by the treatment. Two integrins (α6 and β5), four molecules of the cadherin superfamily, including E-cadherin gene (*CDH1*), and claudin 1, a major cell adhesion molecule in tight junctions, displayed a similar pattern of modulation by gefitinib and cetuximab. Interestingly, the expression of two genes coding for proteins involved in an important apoptotic pathway for tumor cells, such as *FAS* and *TRAIL*, and two major angiogenic factors (*VEGF* and *PDGFA*), were modified by the treatment with both anti-EGFR agents.

On the basis of t test statistical analysis, we identified 45 genes differentially expressed after treatment with gefitinib or cetuximab. Genes involved in multiple processes were found, including genes related to cell proliferation and differentiation (*CDK7*, *EMS1*, *SMARCA5*), transcription (*E2F5*, *CRSP6*, *TRAF3*), DNA synthesis and repair (*TDG*, *RECQL*), angiogenesis (*ENG*), signaling molecules (*JAK1*, *PI3KCD*), cytoskeleton organization (*TLN1*, *MFAP1*), and tumor invasion and metastasis (*PLAU*; Table 6). We validated the expression levels of selected genes obtained in array experiments by semiquantitative reverse transcription-PCR (*CDH1*, *EMS1*, *PLAU*, and *PI3KCD*) and by quantitative real-time PCR (*TRAIL*; Fig. 8).

DISCUSSION

In the present study, we have observed that the combination of cetuximab and gefitinib is synergistic both *in vitro* and *in vivo*. The *in vitro* studies suggest that the synergism is limited to cell lines that have medium-to-high levels of EGFR expression and that are sensitive to both single-agent cetuximab and ge-

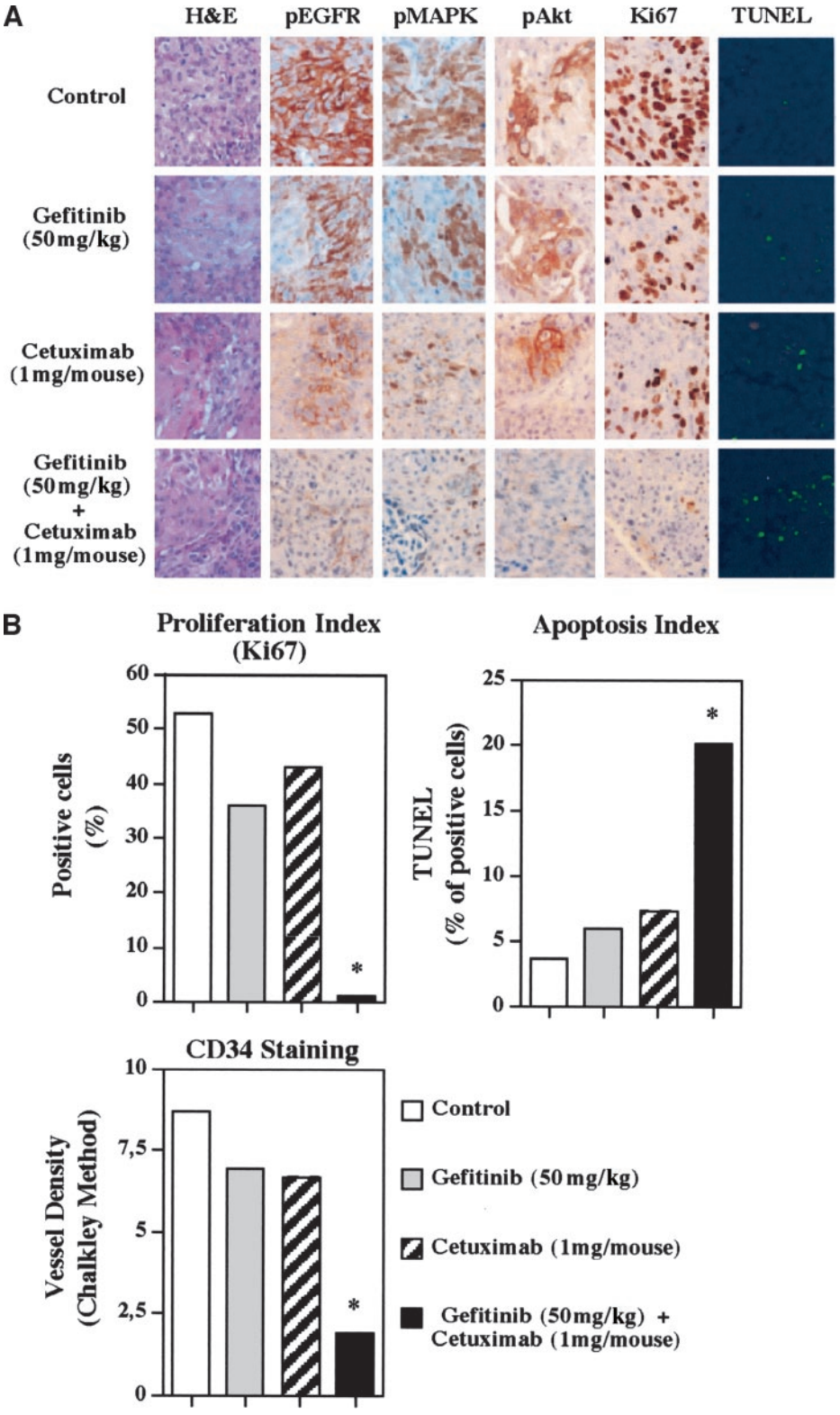

Fig. 7 Tissue-based studies of A431 tumor xenografts treated with gefitinib (50 mg/kg/d), cetuximab (1 mg per mouse twice a week) or the combination of both (from study design I), *A*, immunohistochemical analysis of tumor cells stained with hematoxylin and eosin (*H&E*), anti-phospho-EGFR, anti-phospho-MAPK, anti-phospho-Akt, anti-Ki67 nuclear antigen, and apoptosis by TUNEL (×400). *B*, quantification of proliferation index (Ki67), apoptosis index (TUNEL), and CD34 vessel staining (Chalkley Method). Results are expressed as percentage of positive cells for each marker (Mann–Whitney *U* test: *, $P < 0.01$).

Table 5 Genes regulated by gefitinib and cetuximab in A431 cells

Gene symbol	Gefitinib fold	Cetuximab fold	Description
Cell cycle/DNA replication			
PRIM1	−3.33	−2.32	*Primase, polypeptide 1 (49 kd)*
CCNH	−2.50	−2.20	*Cyclin H*
CCNC	−2.43	−2.25	*Cyclin C*
TOP1	−2.20	−2.40	*Topoisomerase (DNA) 1*
TOP2A	−2.17	−2.08	*Topoisomerase (DNA) II α (170 kd)*
CCNA2	−2.16	−2.20	*Cyclin A2*
Cell adhesion			
PCDHB5	−2.27	−2.27	*Protocadherin β 5*
ITGA6	−2.20	−2.17	*Integrin, α 6*
ITGB5	−2.12	−2.27	*Integrin, β 5*
EMP1	−2	−4	*Epithelial membrane protein 1*
PCDHA10	2.06	2.01	*Protocadherin α 10*
CLDN1	2.33	2.24	*Claudin 1*
PCDHA12	2.61	2.15	*Protocadherin α 12*
CDH1	2.92	2.96	*Cadherin 1, type 1, E-cadherin (epithelial)*
Cell growth			
VEGF	−3.80	−4.65	*Vascular endothelial growth factor*
LTBP2	−2.17	−2.32	*Latent transforming growth factor β binding protein 2*
PDGFA	−2.08	−2.04	*Platelet-derived growth factor α polypeptide*
GADD45B	2.29	2.16	*Growth arrest and DNA-damage-inducible, β*
BST2	2.42	2.28	*Bone marrow stromal cell antigen 2*
IGFBP3	2.63	2.50	*Insulin-like growth factor binding protein 3*
Cell death related			
TNFRSF6	−2.81	−3.70	*Tumor necrosis factor receptor superfamily, member 6 (FAS)*
TNFSF10	2.74	2.44	*Tumor necrosis factor receptor (ligand) superfamily member 10 (TRAIL)*
Transcription related			
BCL3	−3.70	−2.31	*B-cell CLL/lymphoma 3*
SIX6	−3.22	−2.63	*Sine oculis homeobox (Drosophila) homolog 6*
ZFP37	−2.63	−2.86	*Zinc finger protein homologous to Zfp37 in mouse*
MATR3	−2.50	−2.27	*Matrin 3*
LRRC2	−2.43	−2.17	*Leucine-rich-repeat-containing 2*
PBX2	−2.17	−2.22	*Pre-B-cell leukemia transcription factor 2*
TCF6L1	−2.04	−2.63	*Transcription factor 6-like 1 (mitochondrial TF 1-like)*
HDAC2	−2	−2.50	*Histone deacetylase 2*
XBP1	−2.04	−2.2	*X-box binding protein 1*
TRAP95	2.03	2.14	*Thyroid hormone receptor-associated protein, 95 kd subunit*
HDAC7A	2.05	2.37	*Histone deacetylase 7A*
POU5F1	2.16	2.80	*POU domain, class 5, transcription factor 1*
Signal transduction			
NXPH1	−2.98	−4	*Neurexophilin 1*
ILRAP	−2.50	−3.57	*Interleukin1 receptor accessory protein*
PRKRIR	−2.25	−2.35	*Protein-kinase, interferon-inducible dsrna dependent inhibitor*
TEK	−2.22	−4	*TEK tyrosine kinase*
MAPK8IP3	2.03	2.17	*Mitogen-activated protein kinase 8 interacting protein 3*
MAP3K10	2.10	2.17	*Mitogen-activated protein kinase kinase kinase 10*
IL1RN	2.65	3.69	*Interleukin1 receptor antagonist*
Transporter			
ARF5	−2.56	−3.33	*ADP-ribosylation factor 5*
ARF1	2.61	2.12	*ADP-ribosylation factor 1*
Cytoskeleton			
TUBB5	−8.19	−7.7	*Tubulin, β 5*
CAPZA1	−2.70	−2.56	*Capping protein (actin filament), muscle Z-line, α 1*
KRT19	2.37	4.48	*Keratin 19*
Metabolism			
LYPLA1	−2.22	−2.7	*Lysophospholipase 1*
Basic cellular function			
TBCE	−2.38	−2.08	*Tubulin-specific chaperone E*
VBP1	−2.32	−2.5	*Von Hippel-Lindau binding protein 1*
N33	−2.22	−2.56	*Putative prostate cancer tumor suppressor*
MAN1	−2.12	−2.32	*Integral inner nuclear membrane protein*
Secreted protein			
CTSD	2.55	2.69	*Cathepsin D (lysosomal aspartyl protease)*
SERPINE1	−2.70	−2.63	*Serine (or cysteine) proteinase inhibitor, plasminogen activator inhibitor 1 (PAI-1)*
Miscellaneous			
TSSC3	−5.2	−5.55	*Tumor suppressing subtransferable candidate 3*
PCANAP1	−2.77	−3.92	*Prostate cancer associated protein 1*
P23	−2.63	−2.86	*Unactive progesterone receptor, 23 kd*
TSSC1	2.02	2.31	*Tumor suppressing subtransferable candidate 1*
ANXA8	2.24	2.03	*Annexin A8*
SKI	2.14	2.01	*V-ski avian sarcoma viral oncogene homolog*

Note. This table includes the genes found to be ≥2-fold up-regulated or down-regulated in A431 cells treated with gefitinib or cetuximab with respect to untreated tumor cells.

Table 6 Genes differentially expressed in A431 cells treated with gefitinib or cetuximab

Gene symbol	Gefitinib fold	Cetuximab fold	Description
Cell cycle			
MCM5	−1.77	1.28	*Minichromosome maintenance deficient 5, cell division cycle 46*
PPP1CC	1.19	−1.57	*Protein phosphatase 1, catalytic subunit, γ isoform*
Cell death			
CARD12	−1.57	−2.42	*Caspase recruitment domain family, member 12*
Transcription related			
E2F5	−1.28	−1.66	*E2F transcription factor 5, p130-binding*
EIF4A2	1.84	−1.14	*Eukaryotic translation initiation factor 4A, isoform 2*
CRSP6	−1.52	−2.32	*Cofactor required for Sp1 transcriptional activation, subunit 6,77kDa*
TRAF3	−1.43	−1.91	*TNF receptor-associated factor 3*
TP53BPL	−1.22	−1.83	*Tumor protein p53-binding protein*
HOXC10	−2.59	−1.32	*Homeobox protein Hox-C10*
HOXD8	−1.69	1.25	*Homeobox protein Hox-D8*
ZNFN1A1	−1.92	1.29	*Zinc finger protein, subfamily 1A, 1 (Ikaros)*
ZNF212	−1.08	1.58	*Zinc finger protein 212*
RRN3	−1.10	−1.71	*ribosomal DNA (rDNA) transcription*
Cell proliferation/differentiation			
EMS1	−1.49	1.39	*Ems1 sequence (mammary tumor and squamous cell carcinoma-associated (p80/85 src substrate)*
CDK7	−1.02	−1.65	*Cyclin-dependent kinase 7*
SMARCA5	−1.70	−2.24	*SWI/SNF related, matrix associated, actin dependent regulator of chromatin, subfamily a, member 5*
AMY	−1.48	1.74	*Neuroblastoma (nerve tissue) protein*
PTPN6	−1.75	1.26	*Protein tyrosine phosphatase, non-receptor type 6*
DNA repair			
RECQL	−1.45	−2.50	*RecQ protein-like (DNA helicase Q1-like)*
TDG	−1.48	−1.91	*Thymine-DNA glycosylase*
Oncogene			
NET1	−1.48	−2.67	*Neuroepithelial cell transforming gene 1*
Secreted protein			
PLAU	−1.32	−2.40	*Plasminogen activator, urokinase*
Protein biosynthesis			
PRKR	−2.42	−1.46	*Protein kinase, interferon-inducible double stranded RNA dependent*
PSMD10	−1.25	−1.89	*Proteasome (prosome, macropain) 26S subunit, non-ATPase, 10*
PSMC6	−1.76	−2.45	*Proteasome (prosome, macropain) 26S subunit, ATPase, 6*
Cytoskeleton			
TLN1	1.04	1.95	*Talin 1*
MFAP1	1.04	−1.56	*Microfibrillar-associated protein 1*
Extracellular matrix			
COL4A1	1.56	2.07	*Collagen, type IV, alpha 1*
Cell signaling			
PIK3CD	−1.35	1.50	*Phosphoinositide-3-kinase, catalytic, δ polypeptide*
NTRK2	−1.44	1.45	*Neurotrophic tyrosine kinase, receptor, type 2*
JAK1	−1.43	1.28	*Janus kinase 1 (a protein tyrosine kinase)*
Immune response			
IGHG3	−1.49	1.22	*Immunoglobulin heavy constant γ 3 (G3m marker)*
CSF1	−1.42	1.35	*Colony stimulating factor 1 (macrophage)*
Metabolism			
ENO1	−2.05	1.25	*Enolase 1, (α)*
GSTP1	1.02	1.64	*Glutathione S-transferase π*
OAT	−1.68	−2.19	*Ornithine aminotransferase (gyrate atrophy)*
Angiogenesis			
ENG	2.24	9.63	*Endoglin (Osler-Rendu-Weber syndrome 1)*
Basic cellular function/ Miscellaneous			
ITM2B	−1.17	−1.84	*Integral membrane protein 2B*
CAPZA2	−1.39	−2.22	*Capping protein (actin filament) muscle Z-line, α 2*
HSPB2	−1.34	1.55	*Heat shock 27kDa protein 2*
CLU	−1.03	−1.56	*Clusterin (complement lysis inhibitor, SP-40, 40, sulfated glycoprotein 2)*
SOX22	−1.41	1.25	*SOX-12 protein (SOX-22 protein)*
DKFZP564O0463	−1.59	−2.92	*HSPC064 protein*
ESTs	−1.68	−1.16	*EST, AI247680*
ESTs	−1.62	−1.01	*EST, Moderately similar to chemokine receptor D6 [H. sapiens], g4665651*

Note. This table includes the genes that were differentially expressed in A431 cells treated with gefitinib or cetuximab. The genes were considered differentially expressed if they had an unadjusted *P* value of ≤0.03 (*t* test).

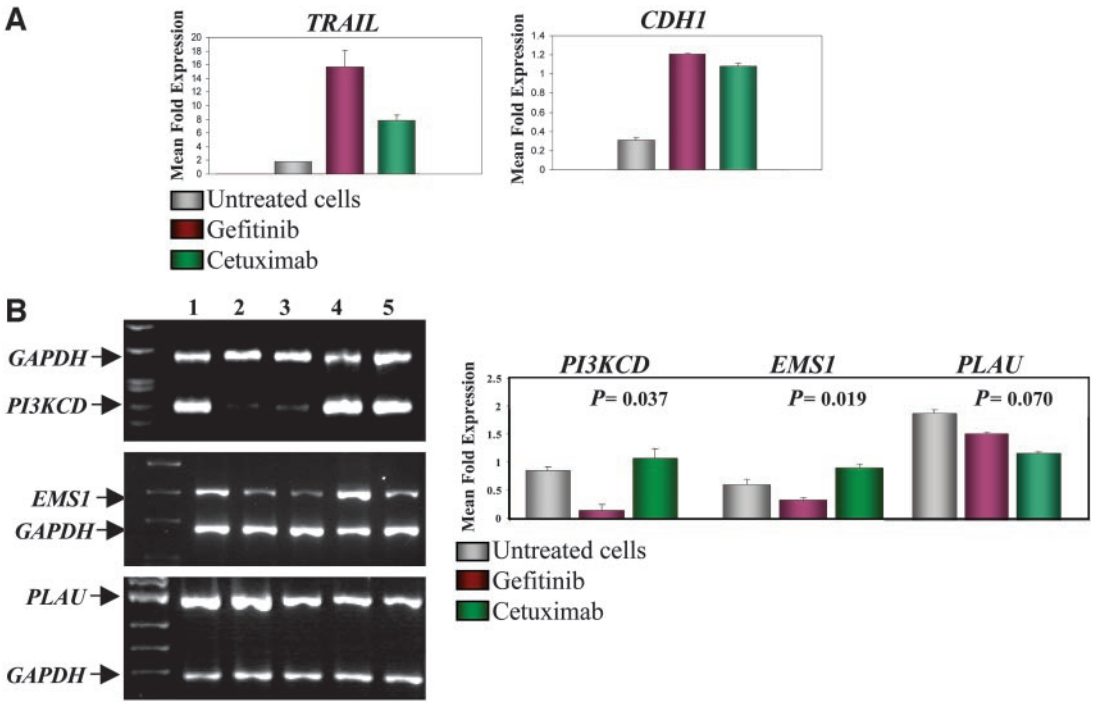

Fig. 8 A, arrays data validation of selected genes (*TRAIL* and *CDH1*) up-regulated in A431 cells treated with gefitinib and cetuximab. *B*, *PI3KCD*, *EMS1* and *PLAU* genes were analyzed from cDNA obtained after RNA extraction of untreated cells (*Lane 1*), cells treated with gefitinib 0.1 μmol/L (*Lane 2*) or 1 μmol/L (*Lane 3*), and cells treated with cetuximab 0.5 nmol/L (*Lane 4*) or 5 nmol/L (*Lane 5*). *Three P values across top of bar graph*, statistical significance between gefitinib and cetuximab treatment for each of the analyzed genes; *columns in bar graph*, for gefitinib (*red*) and cetuximab (*green*), the mean value of both doses for each agent.

fitinib. The antitumor effects with the combination were observed, although maximally inhibitory single-agent dosing was used. In the A431 xenograft model, the combined treatment was synergistic in all of the experiments and resulted in a high rate of complete and persistent tumor regressions. The lack of recurrence after months of follow-up in the combination groups is an important finding because, as previously reported and confirmed in the present study, the highest doses of cetuximab and gefitinib always result in tumor regrowth on treatment discontinuation (25, 26).

We explored potential mechanisms underlying the observed synergy of the combination. On one hand, the two agents given together exerted a superior blockade on EGFR activation and downstream signaling, which resulted in a greater degree of inhibition of phosphorylation of the receptor, MAPK and Akt. These effects were seen both *in vitro* and *in vivo*. In addition to analyzing these well-known EGFR signaling pathways, we took a broader approach, that is, with cDNA microarrays. In total, there were 59 genes that were regulated in the same way and with similar magnitude (≥2-fold up- or down-regulated with respect to untreated cells) by the two treatments (20 up-regulated and 39 down-regulated). In this set of genes, an important control of the assay was provided by the observed down-regulation of *VEGF* with both agents, a well known effect of EGFR inhibition (27–29). In our studies, we observed a several-fold decrease of tumor vascularization in the combination group, which could be a consequence of *VEGF* repression. We also observed up-regulation of genes coding the cell adhesion molecules cadherin E and claudin 1. EGFR activation leads to the inactivation of the E-cadherin/catenin complex in cancer cells, which appears to be critical for control of intercellular adhesion (30) It is, therefore, not surprising to observe up-regulation of *E-cadherin* as a consequence of EGFR blockade (31). The up-regulation of *claudin-1*, a structural component of the tight junctions, it is also fitting with the observation that the pharmacological inhibition of MAPK kinase (MEK1) in *ras*-transformed cells results in restoration of claudin-1 function and the assembling of tight cell junctions (32). Another yet-undescribed effect of EGFR blockade with both agents was the up-regulation of the tumor necrosis factor (TNF)-related apoptosis-inducing ligand (*TRAIL*) gene that could potentially be related to the enhanced apoptosis that we observed (33). This finding could be complementary to the previously reported TRAIL-independent induction of caspase-8 with cetuximab (34).

We identified 45 genes differentially expressed after treatment with gefitinib or cetuximab, including genes related to cell proliferation and differentiation, transcription, DNA synthesis and repair, angiogenesis, signaling molecules, cytoskeleton organization, and tumor invasion and metastasis. We found of particular interest that gefitinib and cetuximab significantly reduced the expression of *PLAU*, the gene coding for urokinase-type plasminogen activator (uPA). uPA, an extracellular serine protease, functions in conjunction with cell surface receptor uPAR in the creation of an active plasmin protease; the uPA system has been proposed to play a key role during cell invasion and it has been demonstrated that increased uPA and uPAR

expression in many tumor types predicts a poor patient prognosis (35). Previous studies have demonstrated that TGF-α, an EGFR ligand, increases uPA in cultured human keratinocytes (36), and, more recently, it has been demonstrated that the EGFR plays a central role in mediating cellular growth signals initiated by uPAR and integrins (37). The uPAR/integrin complex activates the EGFR and MAPK in a ligand-independent fashion, and it has been proposed that this could be a mechanism of resistance to anti-EGFR monoclonal antibodies because they prevent ligand-mediated receptor activation, but not ligand-independent EGFR signaling (37). The finding that uPA decreases markedly with cetuximab may invalidate this hypothesis and suggest a previously undescribed mechanism of action of anti-EGFR therapies. Interestingly, another of the genes differentially expressed between cells treated with gefitinib or cetuximab was *EMS1*. *EMS1* localizes to chromosomal locus 11q13, a region commonly amplified in breast cancers and squamous cell carcinomas of the head and neck (38). *EMS1* codes for cortactin, a protein that seems to play an important role in regulating the trafficking of receptor-containing vesicles after EGFR internalization (39). Also, the functional properties of cortactin suggest a link with tumor cell invasion (40). Our preliminary results suggest that targeting the EGFR function by gefitinib and cetuximab treatment might inhibit tumor invasiveness through the uPA and/or cortactin pathways.

Further analysis of the full panel of coregulated and differentially regulated genes may provide a deeper insight into the molecular mechanisms by which gefitinib and cetuximab exert their antitumor effects and may further explain their complementary antitumor activity. At the cellular function level, the effects of the combined treatment were a profound decrease in proliferation and vascularization as well as an enhancement of apoptosis (Fig. 7*B*).

Our results suggest the coexistence of shared and complementary mechanisms of action with these agents that could be the basis for the observed synergism with the combination. In addition, the study of genes that are coregulated by the two classes of agents could lead to the identification of a "receptor-sensitive signature" that would be instrumental to the identification of tumors sensitive to EGFR inhibition in the clinic. The presence of genes differently regulated may also be useful to understand differences in the clinical activity profile with these two agents. On the basis of results of this combination, we have started a clinical study of gefitinib plus cetuximab in patients with advanced EGFR-expressing tumors. In this study we have incorporated, as in other ongoing studies with anti-EGFR agents (11), sequential tumor biopsies to test the applicability of genomic profiling as a predictor tool of benefit to these therapies. If this combined approach turns out to be safe and active, the concept of combined molecular targeting of the EGFR could represent a novel strategy in the field of molecular therapeutics.

REFERENCES

1. Yarden Y, Sliwkowski M. Untangling the ErbB signalling network. Nat Rev Mol Cell Biol 2001;2:127–37.

2. Schlessinger J. Cell signaling by receptor tyrosine kinases. Cell 2000;103:211–25.

3. Mendelsohn J. Blockade of receptors for growth factors: an anticancer therapy–the fourth annual Joseph H Burchenal American Association of Cancer Research Clinical Research Award Lecture. Clin Cancer Res 2000;6:747–53.

4. Mendelsohn J, Baselga J. Status of epidermal growth factor receptor antagonists in the biology and treatment of cancer. J Clin Oncol 2003; 21:2787–99.

5. Fan Z, Lu Y, Wu X, Mendelsohn J. Antibody-induced epidermal growth factor dimerization mediates inhibition of autocrine proliferation of A431 squamous carcinoma cells. J Biol Chem 1994;269:27595–602.

6. Naramura M, Gillies SD, Mendelsohn J, Reisfeld RA, Mueller BM. Therapeutic potential of chimeric and murine anti-(epidermal growth factor receptor) antibodies in a metastasis model for human melanoma. Cancer Immunol Immunother 1993;37:343–9.

7. Anido J, Matar P, Albanell J, et al. ZD1839, a specific epidermal growth factor receptor (EGFR) tyrosine kinase inhibitor, induces the formation of inactive EGFR/HER2 and EGFR/HER3 heterodimers and prevents heregulin signaling in HER2-overexpressing breast cancer cells. Clin Cancer Res 2003;9:1274–83.

8. Moasser MM, Basso A, Averbuch SD, Rosen N. The tyrosine kinase inhibitor ZD1839 ("Iressa") inhibits HER2-driven signaling and suppresses the growth of HER2-overexpressing tumor cells. Cancer Res 2001;61:7184–8.

9. Moulder SL, Yakes M, Muthuswamy SK, Bianco R, Simpson JF, Arteaga C. Epidermal growth factor receptor (HER1) tyrosine kinase inhibitor ZD1839 (Iressa) inhibits HER2/Neu(erb-2)-overexpressing breast cancer cells in vitro and in vivo. Cancer Res 2001;61:8887–95.

10. Bos M, Mendelsohn J, Kim YM, Albanell J, Fry DW, Baselga J. PD153035, a tyrosine kinase inhibitor, prevents epidermal growth factor receptor activation and inhibits growth of cancer cells in a receptor number-dependent manner. Clin Cancer Res 1997;3:2099–106.

11. Tabernero J, Rojo F, Jimenez E, et al. A phase I pharmacokinetic (PK) and serial tumor and skin pharmacodynamic (PD) study of weekly, every 2 weeks or every 3 weeks 1-hour (h) infusion EMD72000, an humanized monoclonal anti-epidermal growth factor receptor (EGFR) antibody, in patients (p) with advanced tumors known to overexpress the EGFR[abstract]. Eur J Cancer 2002;38(Suppl 7):69.

12. Seymour L, Goss G, Stewart D, et al. A translational research study of ZD1839 at a dose of 750 mg in patients with pretreated advanced or metastatic colorectal cancer: NCIC CTG IND.122[abstract]. Ann Oncol 2002;13(Suppl 5):73.

13. Arteaga CL, Winnier AR, Poirier MC, et al. p185c-erbB-2 signal enhances cisplatin-induced cytotoxicity in human breast carcinoma cells: association between an oncogenic receptor tyrosine kinase and drug-induced DNA repair. Cancer Res 1994;54:3758–65.

14. Wu X, Fan Z, Masui H, Rosen N, Mendelsohn J. Apoptosis induced by an anti-epidermal growth factor receptor monoclonal antibody in a human colorectal carcinoma cell line and its delay by insulin. J Clin Investig 1995;95:1897–905.

15. Peng D, Fan Z, Lu Y, DeBlasio T, Scher H, Mendelsohn J. Anti-epidermal growth factor receptor monoclonal antibody 225 up-regulates p27KIP1 and induces G1 arrest in prostatic cancer cell line DU145. Cancer Res 1996;56:3666–9.

16. Wosikowski K, Schuurhuis D, Johnson K, et al. Identification of epidermal growth factor receptor and c-erbB2 pathway inhibitors by correlation with gene expression patterns. J Natl Cancer Inst (Bethesda) 1997;89:1505–15.

17. Filmus J, Pollak MN, Cailleau R, Buick RN. MDA-468, a human breast cancer cell line with a high number of epidermal growth factor (EGF) receptors, has an amplified EGF receptor gene and is growth inhibited by EGF. Biochem Biophys Res Commun 1985;128:898–905.

18. Vincent PW, Bridges AJ, Dykes DJ, et al. Anticancer efficacy of the irreversible EGFr tyrosine kinase inhibitor PD 0169414 against human tumor xenografts. Cancer Chemother Pharmacol 2000;45:231–8.

19. Albanell J, Codony-Servat J, Rojo F, et al. Activated extracellular signal-regulated kinases: association with epidermal growth Factor receptor/transforming growth factor alpha expression in head and neck squamous carcinoma and inhibition by anti-EGF receptor treatments. Cancer Res 2001;61:6500–10.

20. Ono K, Tanaka T, Tsunoda T, et al. Identification by cDNA microarray of genes involved in ovarian carcinogenesis. Cancer Res 2000;60:5007–11.

21. Tracey L, Villuendas R, Ortiz P, et al. Identification of genes involved in resistance to interferon-α in cutaneous T-cell lymphoma. Am J Pathol 2002;161:1825–37.

22. Moreno-Bueno G, Sanchez-Estevez C, Cassia R, et al. Differential gene expression profile in endometrioid and nonendometrioid endometrial carcinoma: STK15 is frequently overexpressed and amplified in nonendometrioid carcinomas. Cancer Res 2003;63:5697–702.

23. Chou TC, Talalay P. Quantitative analysis of dose-effect relationships: the combined effects of multiple drugs or enzyme inhibitors. Adv Enzyme Regul 1984;22:27–55.

24. Yokoyama Y, Dhanabal M, Griffioen AW, Sukhatme VP, Ramakrishnan S. Synergy between angiostatin and endostatin: inhibition of ovarian cancer growth. Cancer Res 2000;60:2190–6.

25. Wakeling AE, Guy SP, Woodburn JR, et al. ZD1839 (Iressa): an orally active inhibitor of epidermal growth factor signaling with potential for cancer therapy. Cancer Res 2002;62:5749–54.

26. Goldstein NI, Prewett M, Zuklys K, Rockwell P, Mendelsohn J. Biological efficacy of a chimeric antibody to the epidermal growth factor receptor in a human tumor xenograft model. Clin Cancer Res 1995;1:1311–8.

27. Petit AM, Rak J, Hung MC, et al. Neutralizing antibodies against epidermal growth factor and ErbB-2/neu receptor tyrosine kinases down-regulate vascular endothelial growth factor production by tumor cells in vitro and in vivo: angiogenic implications for signal transduction therapy of solid tumors. Am J Pathol 1997;151:1523–30.

28. Ciardiello F, Caputo R, Bianco R, et al. Inhibition of growth factor production and angiogenesis in human cancer cells by ZD1839 (‘Iressa’), a selective epidermal growth factor receptor tyrosine kinase inhibitor. Clin Cancer Res 2001;7:1459–65.

29. Bockhorn M, Tsuzuki Y, Xu L, Frilling A, Broelsch CE, Fukumura D. Differential vascular and transcriptional responses to anti-vascular endothelial growth factor antibody in orthotopic human pancreatic cancer xenografts. Clin Cancer Res 2003;9:4221–6.

30. Jawhari AU, Farthing MJ, Pignatelli M. The E-cadherin/epidermal growth factor receptor interaction: a hypothesis of reciprocal and reversible control of intercellular adhesion and cell proliferation. J Pathol 1999;187:155–7.

31. Al Moustafa AE, Yansouni C, Alaoui-Jamali MA, O’Connor-McCourt M. Up-regulation of E-cadherin by an anti-epidermal growth factor receptor monoclonal antibody in lung cancer cell lines. Clin Cancer Res 1999;5:681–6.

32. Chen Y, Lu Q, Schneeberger EE, Goodenough DA. Restoration of tight junction structure and barrier function by down-regulation of the mitogen-activated protein kinase pathway in ras-transformed Madin-Darby canine kidney cells. Mol Biol Cell 2000;11:849–62.

33. Wang S, El-Deiry WS. TRAIL and apoptosis induction by TNF-family death receptors. Oncogene 2003;22:8628–33.

34. Liu B, Fan Z. The monoclonal antibody 225 activates caspase-8 and induces apoptosis through a tumor necrosis factor receptor family-independent pathway. Oncogene 2001;20:3726–34.

35. Andreasen PA, Kjoller L, Christensen L, Duffy MJ. The urokinase-type plasminogen activator system in cancer metastasis: a review. Int J Cancer 1997;72:1–22.

36. Jensen PJ, Rodeck U. Autocrine/paracrine regulation of keratinocyte urokinase plasminogen activator through the TGF-alpha/EGF receptor. J Cell Physiol 1993;155:333–9.

37. Liu D, Aguirre Ghiso J, Estrada Y, Ossowski L. EGFR is a transducer of the urokinase receptor initiated signal that is required for in vivo growth of a human carcinoma. Cancer Cell 2002;1:445–57.

38. Rodrigo JP, Garcia LA, Ramos S, Lazo PS, Suarez C. EMS1 gene amplification correlates with poor prognosis in squamous cell carcinomas of the head and neck. Clin Cancer Res 2000;6:3177–82.

39. Lynch DK, Winata SC, Lyons RJ, et al. A Cortactin-CD2-associated protein (CD2AP) complex provides a novel link between epidermal growth factor receptor endocytosis and the actin cytoskeleton. J Biol Chem 2003;278:21805–13.

40. Patel AS, Schechter GL, Wasilenko WJ, Somers KD. Overexpression of EMS1/cortactin in NIH3T3 fibroblasts causes increased cell motility and invasion in vitro. Oncogene 1998;16:3227–32.

Clinical Cancer Research

Combined Epidermal Growth Factor Receptor Targeting with the Tyrosine Kinase Inhibitor Gefitinib (ZD1839) and the Monoclonal Antibody Cetuximab (IMC-C225): Superiority Over Single-Agent Receptor Targeting

Pablo Matar, Federico Rojo, Raúl Cassia, et al.

Clin Cancer Res 2004;10:6487-6501.